

Effects of Cross-Correlations in 2D NOE Experiments¹

P.K. Madhu*, R. Christy Rani Grace* and Anil Kumar*[†]

**Department of Physics and [†]Sophisticated Instruments Facility
Indian Institute of Science, Bangalore - 560 012, INDIA*

Contents

I. Introduction	115
II. Theory	116
1. Net effect due to dipolar cross-correlations in a homonuclear three spin system	118
III. Conclusions	122
IV. References	123

I. Introduction

The development of two dimensional Fourier transform NMR techniques by Professor Ernst during the Seventies and Eighties created a revolution in the study of biomolecules by NMR. The ubiquitous COSY experiment and its many variants, especially the DQFC and TOCSY experiments made it possible to obtain assignments of resonances of molecules containing several hundreds of protons - a task which was considered "impossible" before the development of 2D NMR. Similarly the impact of the 2D NOE experiment was "electrifying". It made it possible to obtain the structures of biomolecules in solution, a task which was considered "very difficult" before the application of this experiment (1-5). The revolutionary developments of Fourier transform NMR spectroscopy in one and multidimensions by Professor Ernst, with literally hundreds of new experiments developed by him during these two decades, leading to an explosion of research in this area by many workers, have culminated in his receiving the 1991 Nobel Prize in Chemistry.

The success of the 2D NOE experiment has made it an "object-la-focus" on which much attention has been paid. In order to extract as much information as possible from this experiment, it is performed in the realm of the initial-rate approximation, build-up

curves and long mixing times, subjecting the data respectively to the two-spin approximation, build-up rates and full relaxation-matrix analyses. Several attempts are underway to obtain "accurate-distances" (not just distance estimates) from the 2D NOE data. Simultaneously there have been many concerns regarding the systematic errors in the distance estimates from 2D NOE data. These are, effects of internal motions (6-9), anisotropy of motion (10-13), spin diffusion (14-19), sources of relaxation other than intra-molecular dipolar interactions, and cross-correlations between different pathways of relaxation of a spin. While many attempts are underway to include the effects of internal motions, anisotropy of reorientation, spin diffusion and other relaxation processes, cross-correlations present somewhat of an insurmountable problem. The problem, as succinctly pointed out by Bull (20), is that if one wants to include cross-correlations for N number of relaxation coupled spins, the dimension of the relaxation matrix goes up exponentially to $2^N \times 2^N$ as against a linear $N \times N$ increase if one neglects cross-correlations. For example, for 10 relaxation coupled spins one needs a 1024×1024 relaxation matrix with cross-correlations and a 10×10 matrix without cross-correlations. Therefore the question, whether one can discard cross-correlations without making much error, becomes very pertinent. In this paper the effects of cross-correlations

¹Presented in part at 5th Chianti workshop on Magnetic Resonance Nuclear and Electron Relaxation, held at San Miniato, Italy, June 1993.

and their influence in the 2D NOE experiments are examined in some detail, especially with respect to their influence on the net NOE.

II. Theory

The longitudinal relaxation of N relaxation coupled spins is in general described by the rate equation (4)

$$-\frac{d\vec{P}(t)}{dt} = \mathbf{W}(\vec{P}(t) - \vec{P}^0) \quad (1)$$

where $\vec{P}(t)$ is a vector of populations of various levels at a time 't' and \vec{P}^0 is their equilibrium value. \mathbf{W} is the longitudinal relaxation rate matrix. The dimension of \vec{P} is 2^N and that of \mathbf{W} is $2^N \times 2^N$. If one neglects the cross-correlations a simpler rate equation describing the magnetization of each spin is obtained as (14,21)

$$-\frac{d\vec{I}_z(t)}{dt} = \mathbf{R}(\vec{I}_z(t) - \vec{I}_z^0) \quad (2)$$

This later equation is the generalized Solomon's equation in which $\vec{I}_z(t)$ describes the longitudinal magnetization of various spins at time 't', their equilibrium values \vec{I}_z^0 and the rate matrix \mathbf{R} whose diagonal elements describe the self relaxation of a spin and the off-diagonal elements the cross-relaxation

(NOE) of one spin with another. The dimension of I_z is N and that of \mathbf{R} is $N \times N$. Equation 2 is the equation used for most biological studies. It is a part of a bigger equation which is equivalent to eqn. 1, but recast in the language of magnetization modes. One defines, single spin magnetization modes I_{zi} (A_z, M_z, \dots), two spin magnetization modes $2I_{zi}I_{zj}$ ($2A_zM_z, 2A_zX_z, \dots$) and multispin modes up to N . It is then possible to express the population of each level P_i as a linear combination of these magnetization modes. Equation 1 can then be recast in terms of these modes and yields for example for 3 relaxation coupled spins, eqn. 3, where ρ_i and σ_{ij} respectively describe the self-relaxation of spin 'i' and cross-relaxation of spin 'i' with spin 'j', Δ_i^{ij} represents the cross-correlation of CSA of spin 'i' with dipolar interactions of spins 'ij'. and $\delta_i = \delta_{ijik}$ represents the cross-correlation between the dipole vectors of spins 'ij' and 'ik' (22-26).

From eqn. 3 it is seen that modes of different order are connected purely by cross terms between different relaxation pathways of a spin, the so called cross-correlation terms. If cross-correlations were negligible, the relaxation matrix would become block-diagonal and the upper left part of this matrix, which connects the single spin modes (the magnetization of each spin) to each other and which contains only auto-correlation terms, would yield eqn. 2.

$$-\frac{d}{dt} \begin{bmatrix} A_z \\ M_z \\ X_z \\ 2A_zM_z \\ 2A_zX_z \\ 2M_zX_z \\ 4A_zM_zX_z \end{bmatrix} = \begin{bmatrix} \rho_A & \sigma_{AM} & \sigma_{AX} & \Delta_A^{AM} & \Delta_A^{AX} & 0 & \delta_A \\ \sigma_{AM} & \rho_M & \sigma_{MX} & \Delta_M^{AM} & 0 & \Delta_M^{MX} & \delta_M \\ \sigma_{AX} & \sigma_{MX} & \rho_X & 0 & \Delta_X^{AX} & \Delta_X^{MX} & \delta_X \\ \Delta_A^{AM} & \Delta_M^{AM} & 0 & \rho_{AM} & \delta_A + \sigma_{MX} & \delta_M + \sigma_{AX} & \Delta_A^{AX} + \Delta_M^{MX} \\ \Delta_A^{AX} & 0 & \Delta_X^{AX} & \delta_A + \sigma_{MX} & \rho_{AX} & \delta_X + \sigma_{AM} & \Delta_A^{AM} + \Delta_X^{MX} \\ 0 & \Delta_M^{MX} & \Delta_X^{MX} & \delta_M + \sigma_{AX} & \delta_X + \sigma_{AM} & \rho_{MX} & \Delta_M^{AM} + \Delta_X^{AX} \\ \delta_A & \delta_M & \delta_X & \Delta_A^{AX} + \Delta_M^{MX} & \Delta_A^{AM} + \Delta_X^{MX} & \Delta_M^{AM} + \Delta_X^{AX} & \rho_{AMX} \end{bmatrix} \begin{bmatrix} A_z - A_z^0 \\ M_z - M_z^0 \\ X_z - X_z^0 \\ 2A_zM_z \\ 2A_zX_z \\ 2M_zX_z \\ 4A_zM_zX_z \end{bmatrix} \quad (3)$$

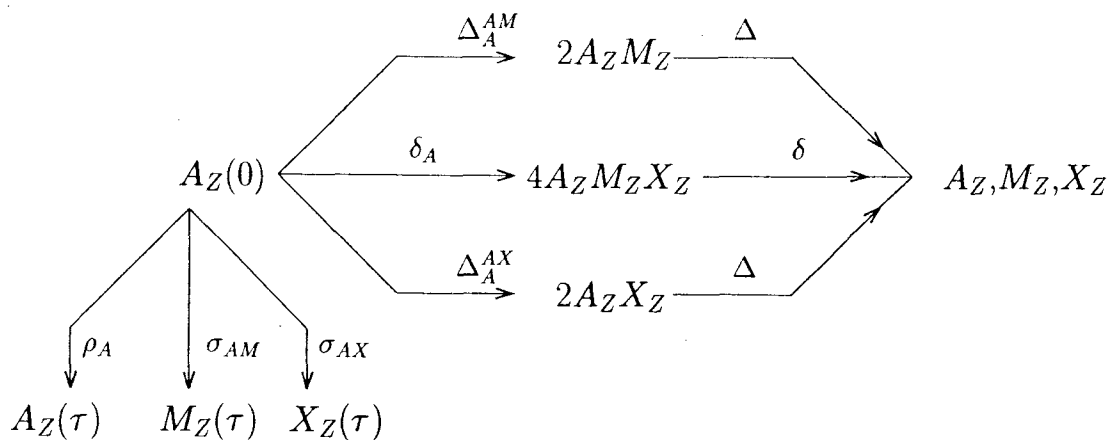


Figure 1.

The presence of multispin modes creates unequal intensities for the various transitions of a spin. For example, the intensities of the four transitions of spin A in an AMX spin system are given by

$$\begin{aligned}
 A_1 &= (1/4)[A_z + 2A_z M_z + 2A_z X_z + 4A_z M_z X_z] \\
 A_2 &= (1/4)[A_z - 2A_z M_z + 2A_z X_z - 4A_z M_z X_z] \\
 A_3 &= (1/4)[A_z + 2A_z M_z - 2A_z X_z - 4A_z M_z X_z] \\
 A_4 &= (1/4)[A_z - 2A_z M_z - 2A_z X_z + 4A_z M_z X_z]
 \end{aligned}
 \quad (4)$$

The net intensity of the spin is the sum of all four transitions, and is given by the single spin mode A_z . If the four transitions are not resolved ($J=0$) or if one uses a 90° measuring pulse (which does not measure the multispin modes) one only sees the net effect. However, the net effect will be different, when cross-correlations are present, from that predicted by eqn. 2. The net effect is independent of the value of J , within the weak coupling limit.

In a 2D NOE experiment on uncoupled or weakly coupled spins using the $[90 - t_1 - 90 - \tau_m - \alpha]$ sequence, each cross-section parallel to F_2 is equivalent to a 1D transient NOE experiment in which the spin (or all the transitions of the spin) on the diagonal, is inverted at $\tau_m = 0$ (27-29). This means that in each cross-section, a single spin mode is created and all the other modes are zero at $\tau_m = 0$. From eqn. 3 it is seen that this single spin mode then evolves, in the initial rate approximation, into single spin modes of other spins (NOE) through cross-relaxation (σ_{ij}), into multispin modes through

cross-correlation (δ_i, Δ_i^{ij}) and also decays by self-relaxation (ρ_i) (Figure 1). At longer mixing times, the multispin modes evolve back into single spin modes of various spins through cross-correlations, giving rise to net NOE and self-relaxation effects due to the presence of cross-correlations.

The presence of multispin modes has been amply demonstrated in several studies: As unequal intensities of various lines of a multiplet in inversion recovery experiments and 2D NOE experiments using a small angle measuring pulse (30-34); in experiments in which the multispin modes are converted into multiple-quantum coherences which are filtered using multiple-quantum-filtered experiments (35-37); and in reverse experiments in which multispin modes are first created and their evolution into single spin modes are monitored (38). One example of the presence of multispin modes in a proton-proton two spin system using inversion recovery experiment is shown in Figure 2. The differential relaxation of the two lines of a spin, indicated by the unequal intensity of the lines during the recovery period, is due to the creation of the two spin mode ($2A_z X_z$). The two spin mode is created here by cross-correlation between the chemical shift anisotropy relaxation (CSA) of the ring protons and their mutual dipolar interaction. Since the magnitude of the CSA of the proton is small, the magnitude of the created two spin mode is small ($< 1.2\%$), in this case.

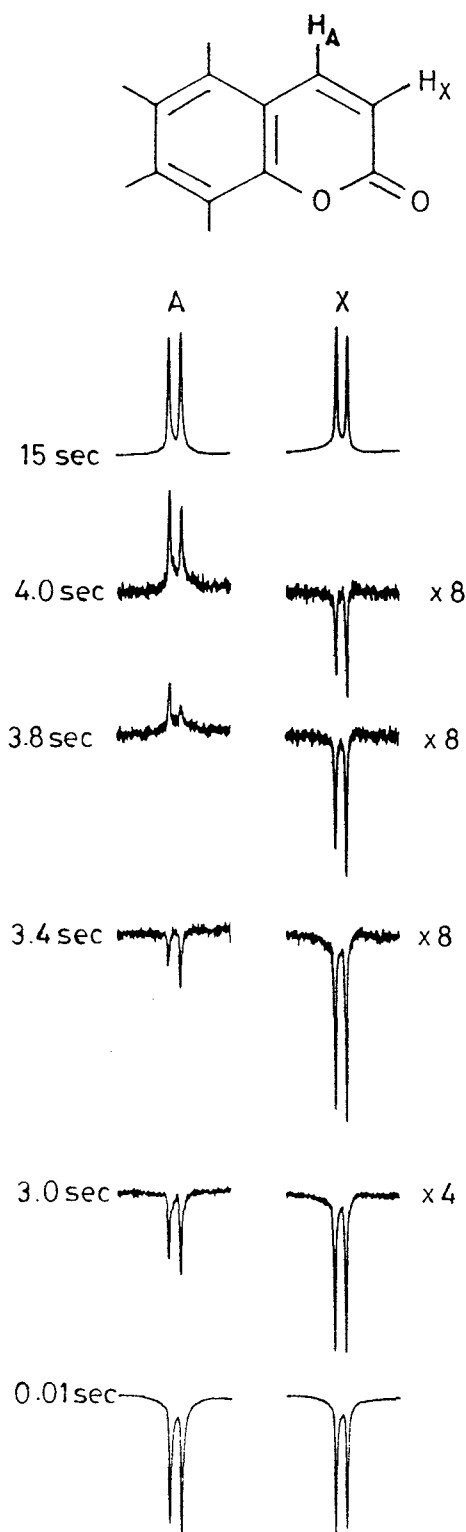


Figure 2: The AX part of the inversion-recovery spectra of coumarin dissolved in CDCl_3 , recorded with a measuring pulse of 20° , for recovery times indicated in the diagram. Some of the spectra are multiplied 4 or 8 times as indicated. The spectra were recorded on an AMX-400 spectrometer.

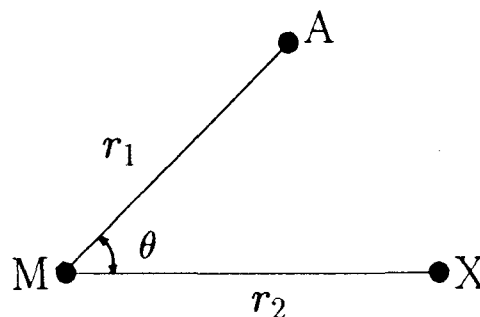


Figure 3.

This paper, on the other hand, concentrates on the net effect arising from the cross-correlations. For this purpose a three spin system is considered, the discussion being restricted to dipole-dipole cross-correlations. It has been earlier shown that there is a significant multiplet effect in such a spin system especially in a linear geometry and that the NOE and the multiplet effect are sensitive to the geometric disposition of the three spins (39).

1. Net effect due to dipolar cross-correlations in a homonuclear three spin system

Three geometries of the relaxation coupled three spin system, without or with weak J couplings (AMX) considered are, (i) equilateral triangle (ii) isosceles triangle with a right angle and (iii) a linear arrangement of the three spins, keeping the distance between 'AM' and 'MX' equal. The magnitude of the geometric factor of the AM-MX dipole-dipole cross-correlation compared to AM-AM auto correlation for the homonuclear system is given by

$$\frac{\delta_M}{\sigma_{AM}} = \frac{1}{2} \left(\frac{r_1}{r_2} \right)^3 (3\cos^2\theta - 1) \quad (5)$$

where r_1 is the distance between A and M spins, r_2 the distance between M and X spins and θ is the angle between these two vectors (Figure 3). For $r_1 = r_2$, this ratio is $-1/8$, $-1/2$, and 1 respectively for equilateral triangle, isosceles triangle and a linear arrangement of the spins. Thus the cross-correlation is extremely sensitive to the geometric disposition of the three spins with the linear arrangement having maximum cross-correlation.

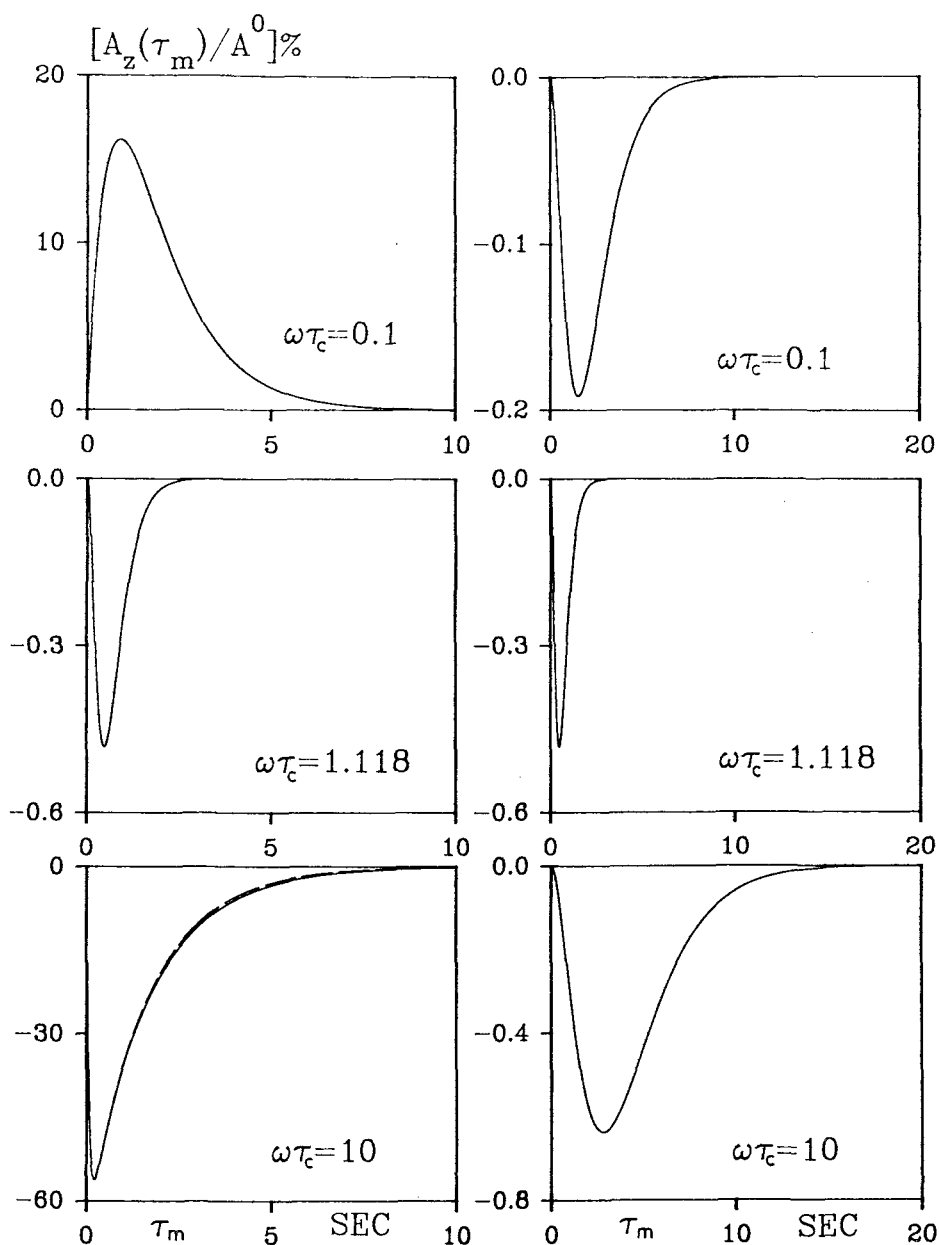


Figure 4: Calculated net NOE in percentage on spin A, after selective inversion of spin M at $\tau_m = 0$ is shown as a function of τ_m for three geometries; (a) equilateral (b) isosceles and (c) linear, for three values of $\omega\tau_c$ in each case. In the left hand diagrams the dashed curves represent the calculated net NOE without cross-correlations and the solid curves with cross-correlations. In the right hand diagrams the difference between these two calculated NOE's are shown by solid curves.

The calculated net NOE on spin A $[A_z(\tau_m)]$ for the selective inversion of spin M (equal to the intensity of AM cross peak in a cross-section parallel to F_2 at the frequency of M spin in a 2D NOE experiment having all the three pulses as 90°) in the three geometries is shown in Figure 4. Also shown in this figure is the calculated net NOE without cross-correlations and the difference between the net NOE calculated with and without cross-correlations. The

net NOE has been calculated for three values of $\omega\tau_c = 0.1, 1.118$ and 10 , in each case. The difference is rather small for the equilateral case ($< 0.7\%$) and isosceles case ($< 6\%$), but significant in linear geometry (up to 8% , 13% and 24% respectively for $\omega\tau_c = 0.1, 1.118$ and 10). The difference builds up at a later point in time since it is a second-order effect.

The presence of this significant error in the net

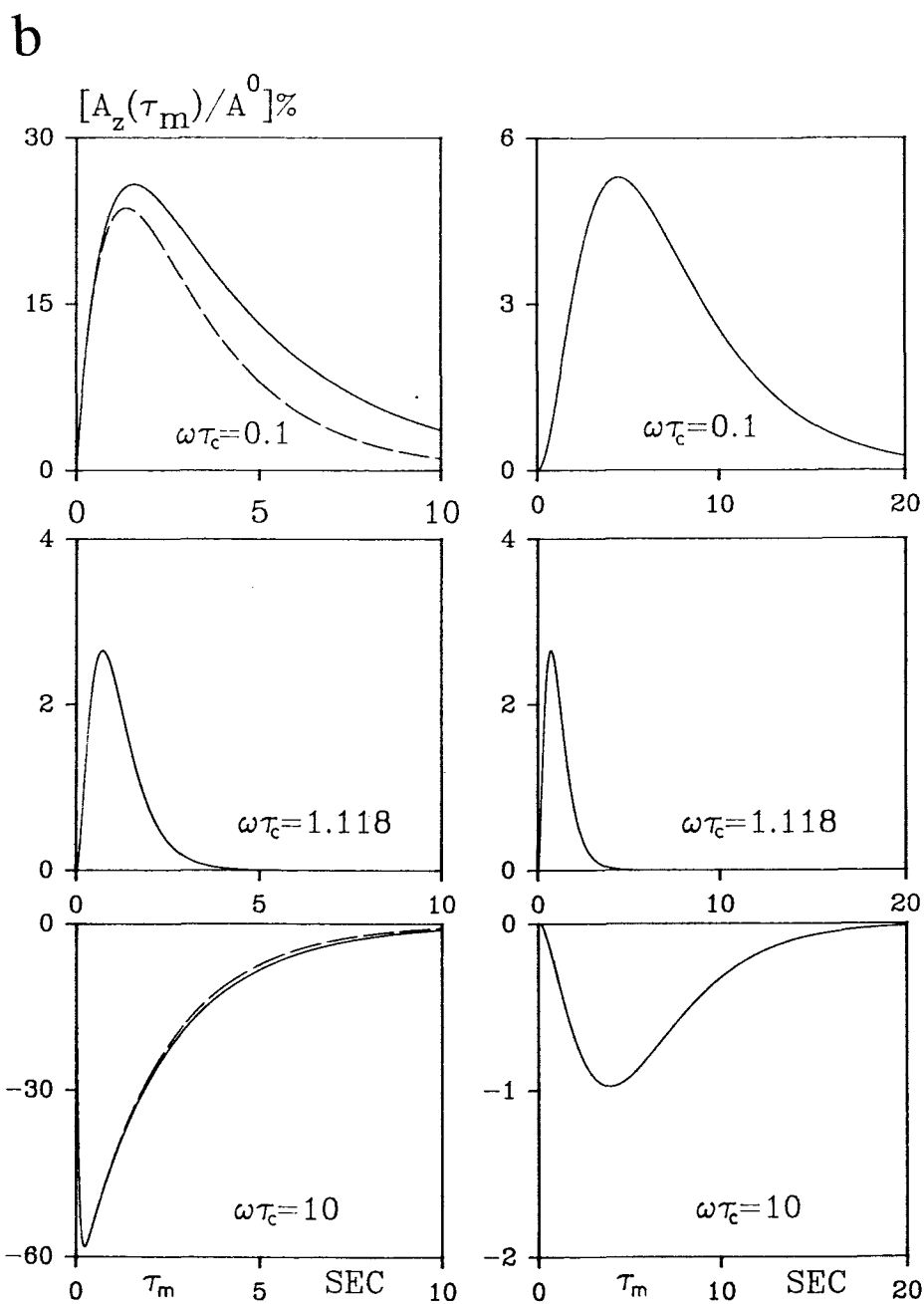


Figure 4: continued.

NOE calculated with and without cross-correlations has a direct consequence in the distance estimation from the 2D NOE data. The neglect of cross-correlations causes a systematic error in the distance measurement. However, the error builds-up at large mixing times since it is due to the second-order effect of cross-correlations. One redeeming factor is that these mixing times are much larger than the mixing times usually employed in 2D NOE experiments. Never-the-less these errors are significant, and are due to opening up of additional relaxation pathways of the spin by the cross-correlations. This is discussed in more detail in the following.

The cross-correlation δ_M transfers some of M magnetization to the three spin order term ($4A_zM_zX_z$) which then leaks to A_z or X_z via δ_A or δ_X respectively or comes back to M_z via δ_M . These additional pathways cause the changes in the net NOE. In equilateral and isosceles triangle cases all the δ 's are small. As a result these additional pathways are insignificant. However in the linear case the geometric factor of the AM-MX cross-correlation is as significant as AM-AM or MX-MX auto-correlation. Thus in the linear case the dominant additional pathway is (δ_M, δ_M) (Figure 5). The NOE from spin M to spin A is affected by two

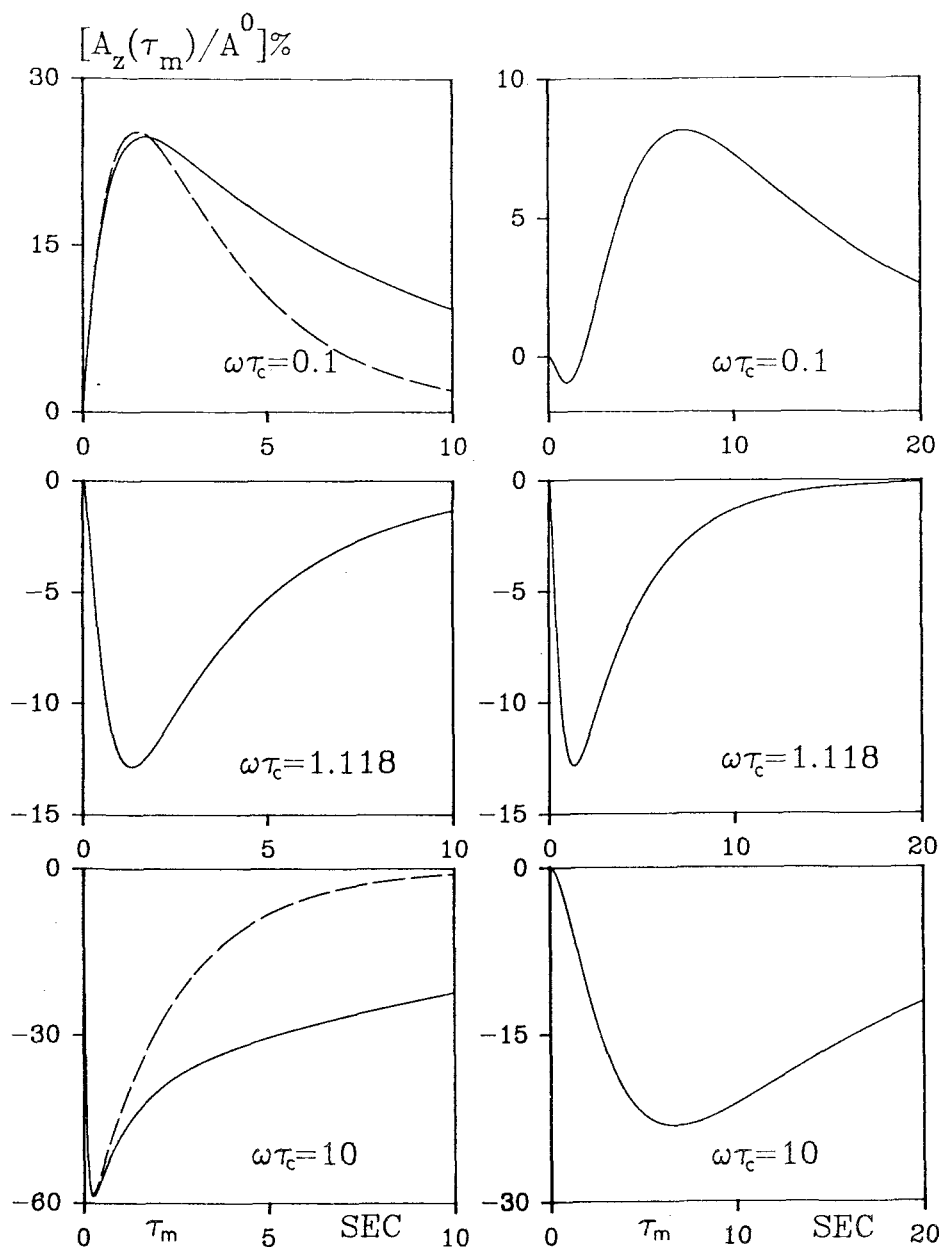


Figure 4: continued.

pathways one involving $(\delta_M, \delta_M, \sigma_{AM})$ path and the other involving (δ_M, δ_A) path (Figure 6). In the $\omega\tau_c = 1.118$ limit $\sigma_{AM} = 0$ and the net NOE to A spin comes only through cross-correlations using the path (δ_M, δ_A) . Since δ_A is small this NOE is small (Figure 4c). However when $\omega\tau_c \gg 1$ ($\omega\tau_c = 10$), σ_{AM} is large along with δ_M and the path $(\delta_M, \delta_M, \sigma_{AM})$ contributes significantly to the net NOE on A and the difference in net NOE calculated with or without cross-correlation is significant (Figure 4c). Identical results are obtained for the X spin in this case due to symmetry and are not shown.

The self-relaxation of spin M is also affected by

the presence of cross-correlations (Figure 7). The self-relaxation of a spin can be monitored as the decay of the diagonal peak in the 2D NOE experiment or by a selective-inversion-recovery experiment. The self-relaxation of spin M shows a very large effect of cross-correlations as has also been pointed out by early workers in this field (40-42). The pathways affecting the self relaxation of spin M are indicated in Figure 8. Of these the dominant path due to cross-correlations is again the path (δ_M, δ_M) . For $\omega\tau_c = 1.118$ the other paths are cut off and this is the only path left.

The NOE from spin A to M and X and its self-

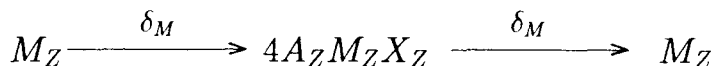


Figure 5.

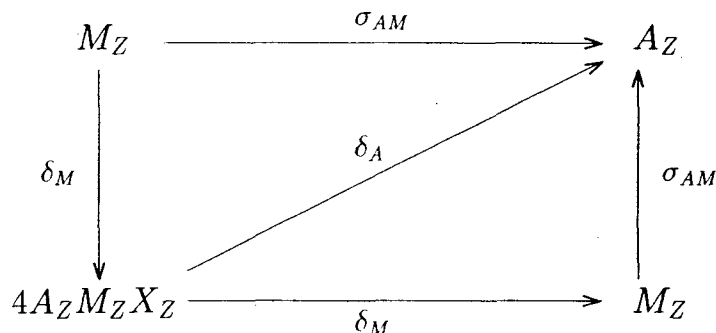


Figure 6.

relaxation is considered next. Since δ_A is small the conversion of A_z to $4A_z M_z X_z$ is weak. Figure 9 shows the net NOE from spin A to M and X for various correlation times. This figure shows that the differences are smaller than Figure 4 but are not negligible. In the short correlation limit ($\omega\tau_c \ll 1$) the net NOE to X is small and the difference with and without cross-correlation is also small. The calculated net NOE on M and X spins without cross-correlations is zero for $\omega\tau_c = 1.118$. The pathways contributing to the net NOE on M and X spins are shown in Figure 10. For $\omega\tau_c = 1.118$ when σ_{AM} and σ_{AX} are zero, the pathways (δ_A, δ_M) and (δ_A, δ_X) exclusively contribute to net NOE on M and X spins respectively. Since both δ_A and δ_X are small compared to δ_M , the error in the net NOE on X is smaller than on M. In the long correlation limit σ_{AM} becomes significant, opening up additional pathways. The dominant pathway using cross-correlations for the net NOE on spin M being $(\sigma_{AM}, \delta_M, \delta_M)$ and for the spin X being $(\sigma_{AM}, \delta_M, \delta_M, \sigma_{MX})$. The difference for both M and X spins comes from (δ_M, δ_M) path and therefore the errors for M and X are almost equal. The self-relaxation of spin A (figure not shown) also shows significant differences for $\omega\tau_c = 10$, the dominant pathway being $(\sigma_{AM}, \delta_M, \delta_M, \sigma_{AM})$ (Figure 10). For $\omega\tau_c = 1.118$ the above pathway is cut off and the errors are due to (δ_A, δ_A) which is weak and hence the error

is small.

These large errors in net NOE arise at rather long mixing times, times which are often not sampled in 2D NOE experiments. In this contrived three spin system, the spin system is isolated from the rest of the spins and in the limit $\omega\tau_c \gg 1$, also gets isolated from the lattice. As a result the magnetization remains within the spin system for a long time. During this long period, the error due to neglect of other pathways builds-up and shows-up at later times. A plausible approach would be to enlarge the spin system and to build-in leakage terms so as to approach the realistic experimental conditions. This is being presently attempted. Isolation of spin systems can however be achieved by selective spin lock (43,44).

III. Conclusions

The error in the calculated net NOE by neglect of cross-correlations while small at small mixing times, is not negligible at larger mixing times, particularly for slow motion limit, the so called biomolecular limit. In this limit, even if one of the cross-correlations at one of the spins is significant, it can affect all the spins to which that particular spin has good cross-relaxation contact. However, in most of the geometries (except linear) dipole-dipole cross-

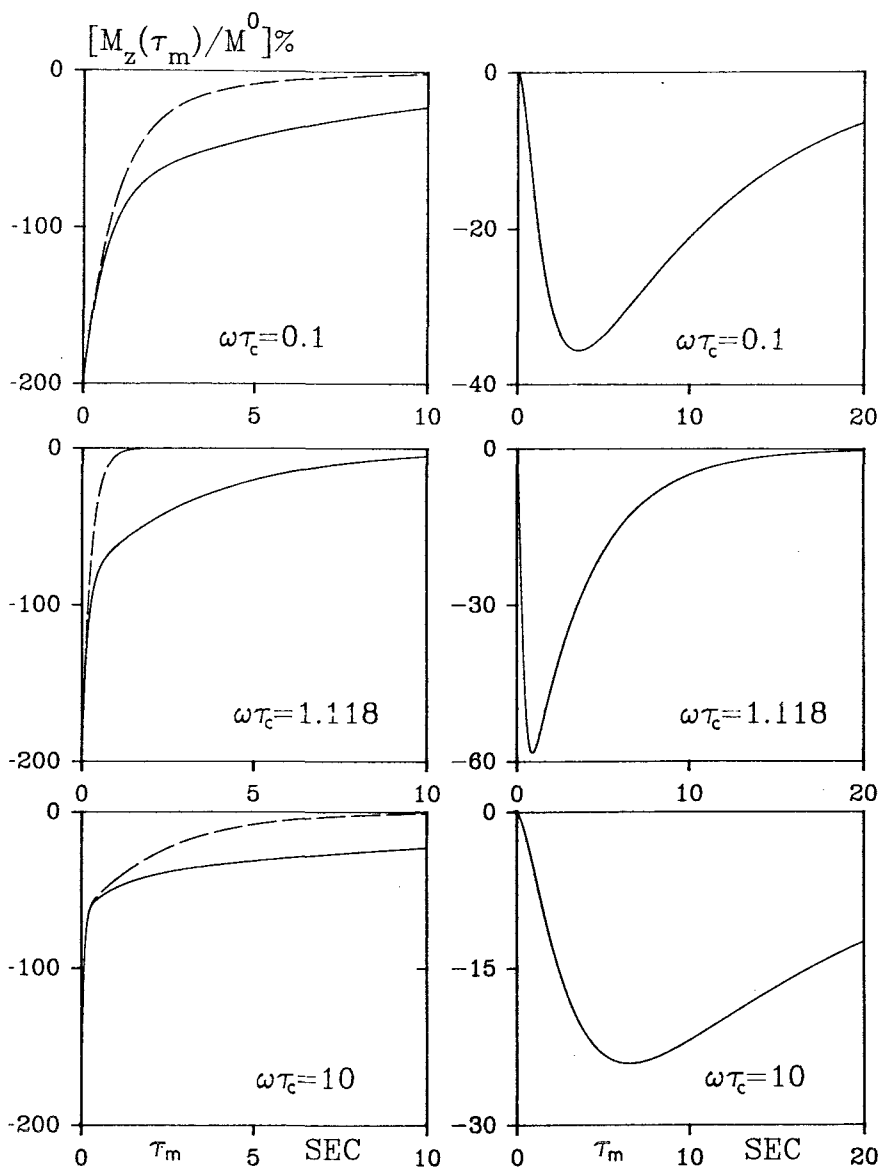


Figure 7: The calculated net magnetization in percentage of spin M is shown as a function of τ_m , after a selective inversion of spin M at $\tau_m=0$ for the linear geometry of the three spins AMX for three different values of $\omega\tau_c$. In the left hand diagrams, the dashed curves represent the calculated magnetization without cross-correlations and the solid curves with cross-correlations. In the right hand diagrams the differences between these two calculated magnetizations are shown by solid curves.

correlations are small. The CSA-dipole cross-correlation for protons are also usually small and perhaps can be ignored. The CSA-dipole cross-correlation is significant for other spin 1/2 nuclei such as ^{19}F , ^{13}C , ^{31}P and ^{15}N and may not be ignored. More work is required to assess whether proton-proton dipole-dipole cross-correlations should be included in biomolecular NOE studies of large molecules.

IV. References

- ¹W. P. Aue, E. Bartholdi and R. R. Ernst, *J. Chem. Phys.* **64**, 2229-2245 (1976).
- ²Anil Kumar, R. R. Ernst and K. Wüthrich, *Biochem. Biophys. Res. Commun.* **95**, 1-6 (1980).
- ³K. Wüthrich, "NMR of Proteins and Nucleic Acids", John Wiley and Sons, New York (1986).

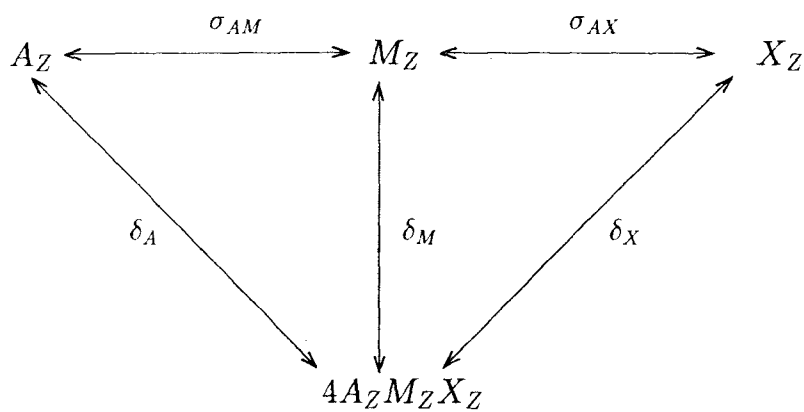


Figure 8.

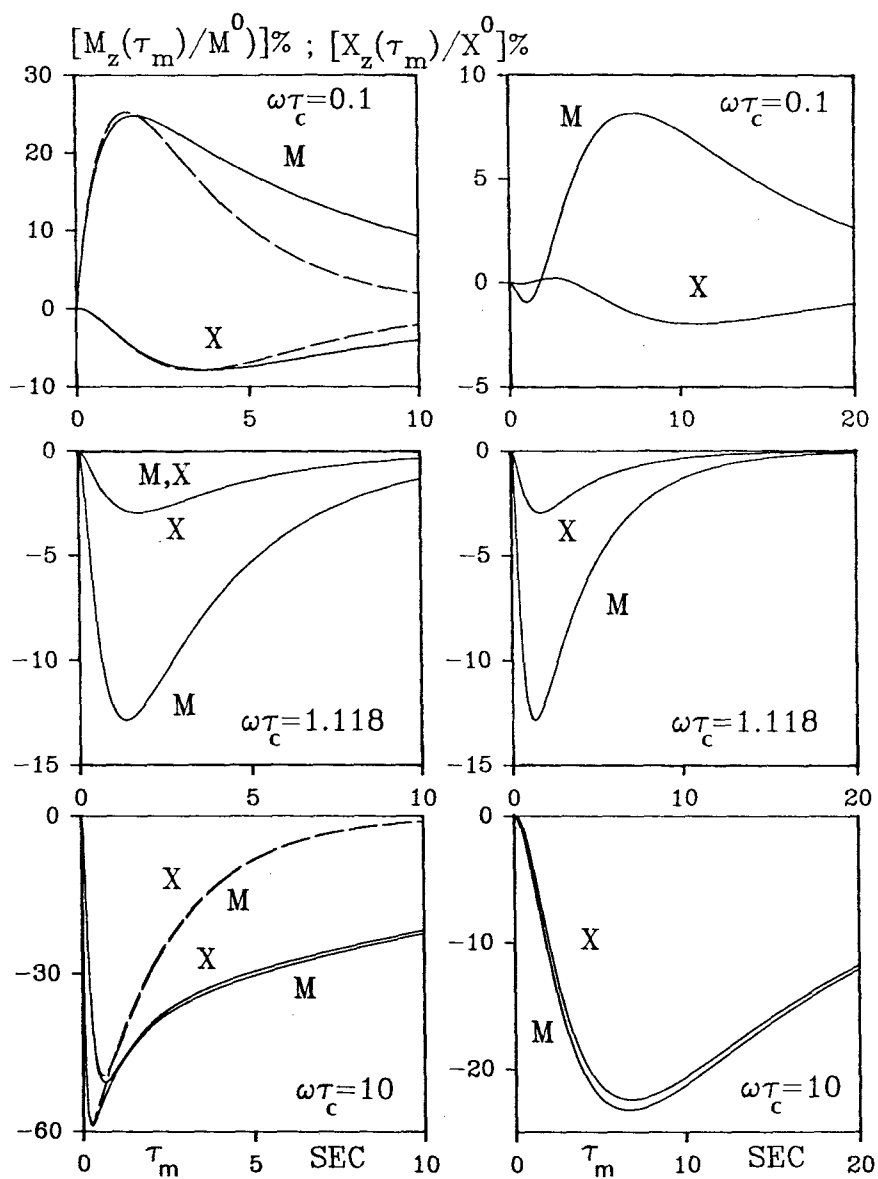


Figure 9: Calculated net NOE in percentage on spins M and X, after a selective inversion of spin A at $\tau_m = 0$, for the linear geometry. The remaining details are same as in Figure 4.

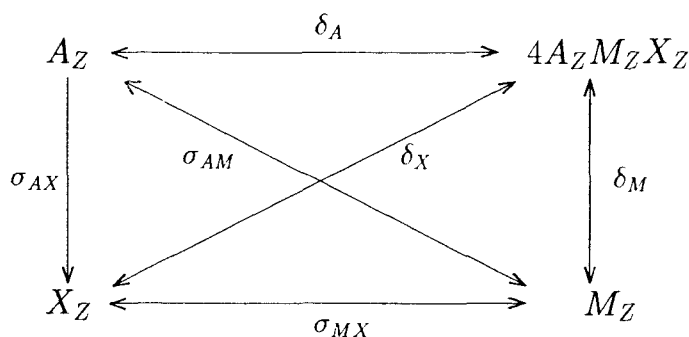


Figure 10.

⁴R. R. Ernst, G. Bodenhausen and A. Wokaun, "Principles of Nuclear Magnetic Resonance in One and Two Dimensions", Oxford Science Publication, London, 1987.

⁵R. R. Ernst, *Angew. Chem. Int. Ed. Engl.* **31**, 805-930 (1992).

⁶D. E. Woessner, *J. Chem. Phys.* **42**, 1855-1859 (1965).

⁷J. W. Keepers and T. L. James, *J. Magn. Reson.* **57**, 402-426 (1984).

⁸L. E. Kay and J. H. Prestegard, *J. Am. Chem. Soc.* **109**, 3829-3835 (1987).

⁹V. V. Krishnan, S. C. Shekar and Anil Kumar, *J. Am. Chem. Soc.* **113**, 7542-7550 (1991).

¹⁰D. E. Woessner, *J. Chem. Phys.* **36**, 1-4 (1963).

¹¹R. L. Vold and R. R. Vold, *Prog. Nucl. Mag. Res. Spec.* **12**, 79-133 (1978)

¹²T. Bluhm, *Mol. Phys.* **47**, 475-486 (1982).

¹³E. Konigsberger and H. Stark, *J. Chem. Phys.* **83**, 2723-2726 (1985).

¹⁴A. Kalk and H. J. C. Berendsen, *J. Magn. Reson.* **24**, 343-366 (1976).

¹⁵Anil Kumar, G. Wagner, R. R. Ernst and K. Wüthrich, *J. Am. Chem. Soc.* **103**, 3654 (1981).

¹⁶E. T. Olejniczak, R. T. Gampe, Jr., and S. W. Fesik, *J. Magn. Reson.* **67**, 28-41 (1986).

¹⁷V. V. Krishnan, N. Murali and Anil Kumar, *J. Magn. Reson.* **84**, 255-267 (1989).

¹⁸A. Majumdar and R. V. Hosur, *J. Magn. Reson.* **88**, 284-304 (1990).

¹⁹V. V. Krishnan, U. Hegde and Anil Kumar, *J. Magn. Reson.* **94**, 605-611 (1991)

²⁰T. E. Bull, *J. Magn. Reson.* **72**, 397-413 (1987).

²¹J. Solomon, *Phys. Rev.* **99**, 559-565 (1955).

²²N. C. Pyper, *Mol. Phys.* **21**, 1-33 (1971).

²³N. C. Pyper, *Mol. Phys.* **22**, 433-458 (1972)

²⁴L. G. Werbelow and D. M. Grant, *Adv. Mag. Res.* **9**, 189-299 (1977).

²⁵D. Canet, *Prog. NMR. Spectrosc.* **21**, 237-291 (1989).

²⁶C. Dalvit and G. Bodenhausen, *Adv. Mag. Res.* **14**, 1-32 (1990).

²⁷R. C. R. Grace and Anil Kumar, *J. Magn. Reson.* **97**, 184-191 (1992).

²⁸R. C. R. Grace and Anil Kumar, *J. Magn. Reson.* **99**, 81-98 (1992).

²⁹R. C. R. Grace and Anil Kumar, *Bulletin Magn. Reson.* **14**, 42-56 (1992).

³⁰G. Jaccard, S. Wimperis and G. Bodenhausen, *Chem. Phys. Lett.* **138**, 601-606 (1987).

³¹C. Dalvitt and G. Bodenhausen, *Chem. Phys. Lett.*, **161**, 554-560 (1989).

³²H. Oschkinat, D. Limat, L. Emsley and G. Bodenhausen, *J. Magn. Reson.* **81**, 13-42 (1989).

³³C. Dalvitt, *J. Magn. Reson.* **95**, 410-416 (1991).

³⁴V. A. Daragan and K. H. Mayo, *Chem. Phys. Lett.* **206**, 393-400 (1993).

³⁵R. Bruschweiler, C. Griesinger and R. R. Ernst, *J. Am. Chem. Soc.* **111**, 8034-8035 (1984).

³⁶C. Dalvitt and G. Bodenhausen, *J. Am. Chem. Soc.* **110**, 7924 (1988).

³⁷S. Wimperis, J. M. Bohlen and G. Bodenhausen, *J. Magn. Reson.* **77**, 589-595 (1988).

³⁸M. Ernst and R. R. Ernst, Fifth Chianti Workshop on Magnetic Resonance, San Miniato, Italy, June, 1993.

³⁹V. V. Krishnan and Anil Kumar, *J. Magn. Reson.* **92**, 293-311 (1991).

⁴⁰V. A. Daragan, T. N. Khazanovich and A. U. Stepanyants, *Chem. Phys. Lett.* **26**, 89-92 (1974).

⁴¹L. G. Werbelow and D. M. Grant, *J. Chem. Phys.* **63**, 544-556 (1975).

⁴²J. Courtieu, P. E. Fagerness, D. M. Grant, *J. Chem. Phys.* **65**, 1202-1205 (1976).

⁴³L. Di. Bari, J. Kowaleswski and G. Bodenhausen, *J. Chem. Phys.* **93**, 7698-7705 (1990).

⁴⁴I. Burghardt, R. Konrat and G. Bodenhausen, *Mol. Phys.* **75**, 467-486 (1992).